

Preparation of a Yb(III)-Incorporated Porous Polymer by Post-Coordination: Enhancement of Gas Adsorption and Catalytic Activity

Hyungwoo Kim, Min Chul Cha, Hyun Woo Park, Ji Young Chang

Department of Materials Science and Engineering, College of Engineering, Seoul National University, Seoul 151-744, Korea

Correspondence to: J. Y. Chang (E-mail: jichang@snu.ac.kr)

Received 21 May 2013; accepted 16 September 2013; published online 10 October 2013

DOI: 10.1002/pola.26962

ABSTRACT: We synthesized a Yb(III)-incorporated microporous polymer (Yb-ADA) and studied its gas adsorption property and catalytic activity. The adamantane-based porous polymer (ADA) was obtained from an ethynyl-functionalized adamantane derivative and 2,5-dibromoterephthalic acid through Sonogashira–Hagihara cross-coupling. ADA had two carboxyl groups which were used for Yb(III) coordination under basic conditions. The Brunauer–Emmett–Teller (BET) surface area of ADA was $970 \text{ m}^2 \text{ g}^{-1}$. As Yb(III) ions were incorporated into ADA, the surface area of the polymer (Yb-ADA) was reduced to $885 \text{ m}^2 \text{ g}^{-1}$. However, Yb-ADA exhibited a significantly enhanced CO_2 adsorption capacity despite the reduction of sur-

face area. The CO_2 uptakes of ADA and Yb-ADA were 1.56 and 2.36 mmol g^{-1} at 298 K, respectively. The H_2 uptake of ADA also increased after coordination with Yb(III) from 1.15 to 1.40 wt % at 77 K. Yb-ADA showed high catalytic activity in the acetalization of 4-bromobenzaldehyde and furfural with trimethyl orthoformate and could be reused after recovery without severe loss of activity. © 2013 Wiley Periodicals, Inc. *J. Polym. Sci., Part A: Polym. Chem.* **2013**, *51*, 5291–5297

KEYWORDS: microporous polymers; networks; microstructure; metal-polymer complexes; catalysis

INTRODUCTION Microporous organic polymers (MOPs) with high surface area and physicochemical stability have attracted considerable attention as gas adsorbents.¹ Compared to traditionally used porous materials such as zeolites and activated carbons, MOPs have an advantage in their synthesis and modification. A variety of building blocks and synthetic methodologies are available for MOPs. In addition, MOPs can be further functionalized using diverse chemical methods which, combined with an appropriately selected building block, will provide the MOPs with the desired property for a specific application.

Several factors govern the gas adsorption behaviors of MOPs, including surface area, pore shape and size, and functionality of the framework. Many efforts to enhance gas adsorption properties of MOPs, particularly for carbon dioxide (CO_2) and hydrogen (H_2), have been reported.^{2–4} For example, several studies demonstrated that an introduction of a polar functional group into an MOP enhanced its CO_2 uptake significantly.³ The effects of metal ions on the gas adsorption of MOPs have also been studied. Lithium ion-doped porous polymers showed an increase in CO_2 and H_2 adsorptions.⁴ High expectations have also been given for metal-containing MOPs for their use in the catalysis of an organic reaction.⁵

In this work, we synthesized a Yb(III)-incorporated microporous polymer (Yb-ADA) from adamantane derivative and 2,5-dibromoterephthalic acid. Yb is an element in the lanthanide series that has the most common oxidation state of +3. An Yb(III) ion normally has a coordination number of six to nine. Depending on coordination conditions, it has labile small molecules such as water as ligands that are easily eliminated to form open metal sites. The cationic open metal sites are known to induce chemical binding with H_2 as well as CO_2 .⁶ Furthermore, Yb(III) complexes are widely used as a Lewis catalyst in organic reactions such as aldol condensation, cyanation, and Michael reaction.⁷ Yb(III) catalysts supported on ion exchange resins were also reported to show a similar catalytic activity.⁸ Herein we present the synthesis of Yb-ADA and its enhanced gas adsorption and catalytic activity.

EXPERIMENTAL

Materials

1,3,5,7-Tetrakis(4-ethynylphenyl)adamantane was synthesized by according to the literature.⁹ All chemicals purchased from Aldrich and TCI were used without any further purification. Other reagent grade solvents were used as received.

Measurement

^1H NMR spectra were recorded on a Bruker Avance 300 spectrometer (300 MHz). Solid state ^{13}C CP/MAS NMR spectra were recorded on a Bruker Avance 400 WB spectrometer (100 MHz) equipped with CP-MAS. Fourier transform infrared (FT-IR) measurements were made on a PERKIN ELMER Spectrum GX I using KBr pellets. Thermogravimetric analyses (TGA) were performed on a TA modulated TGA2050 with a heating rate of $10\text{ }^\circ\text{C}/\text{min}$ under nitrogen. N_2 and CO_2 uptakes were measured by using a Belsorp-Max (BEL Japan) apparatus. Ultra-high purity grade N_2 , H_2 , and CO_2 gases were used for all adsorption measurements. X-ray photoelectron spectroscopy (XPS) measurements were performed on a KRATOS AXIS-Hsi spectrometer equipped with a Mg K_α X-ray source.

Preparation of the Adamantane-Based Porous Polymer

To a solution of 1,3,5,7-tetrakis(4-ethynylphenyl)adamantane (100 mg, 0.19 mmol) and 2,5-dibromoterephthalic acid (80 mg, 0.25 mmol) in DMF (3 mL) were added $\text{PdCl}_2(\text{PPh}_3)_2$ (30 mg, 0.04 mmol) and CuI (10 mg, 0.05 mmol). After degassing for 10 min, diisopropylamine (3 mL) was added dropwise to the reaction mixture. After stirring for 24 h at $90\text{ }^\circ\text{C}$, the precipitated polymer was isolated by filtration and acidified in an aqueous HCl solution (1 N, 10 mL). The resulting polymer was filtered, washed with water, DMF, and acetone, and Soxhlet extracted with MeOH. The polymer was dried in vacuum at $150\text{ }^\circ\text{C}$. Yield: 84%. IR (KBr, cm^{-1}): 3394, 3035, 2933, 2901, 2855, 2198, 1684, 1606, 1507, 1447, 1406, 1359, 1207, 1190, 1117, 1017, 834, 784, 730, 564.

Preparation of the Yb(III)-Coordinated ADA Polymer

Adamantane-based porous polymer (ADA) (60 mg) was dispersed in EtOH (50 mL) and then the pH was adjusted to 8 with an aqueous NaOH solution (2 M). A solution of

ytterbium(III) chloride hexahydrate (103.33 mg, 0.27 mmol) in water (2 mL) was added dropwise to the polymer suspension. After stirring for 10 h at rt, the product was isolated by filtration and washed with water, ethanol, and acetone. The polymer was dried in vacuum at $150\text{ }^\circ\text{C}$. Yield: 92%. IR (KBr, cm^{-1}): 3747, 3620, 3394, 2931, 2855, 2195, 1698, 1636, 1522, 1405, 1363, 1272, 1118, 1017, 835, 779, 675, 569.

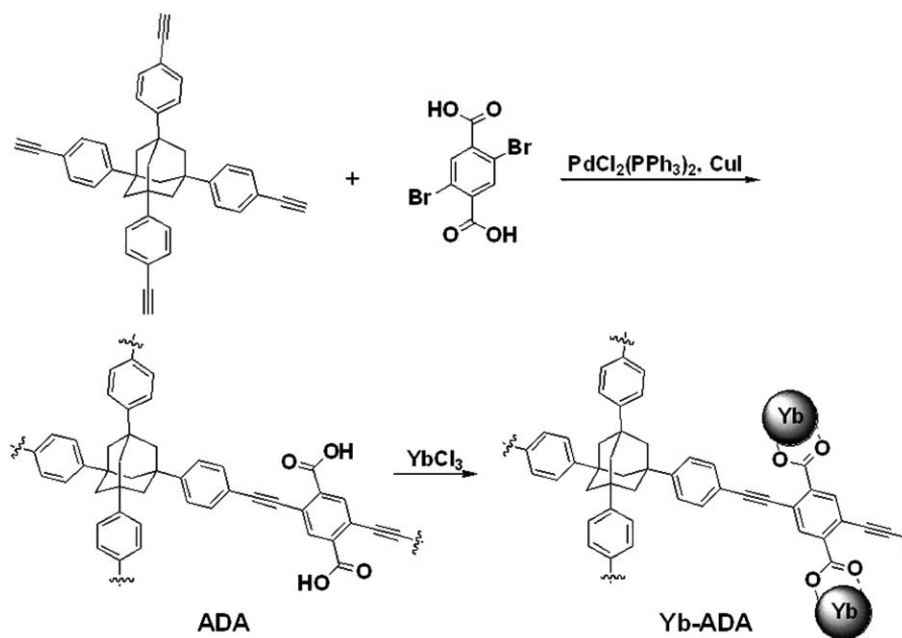
General Procedure for Acetalization

To a solution of an aldehyde (0.1 mmol) and trimethyl orthoformate (0.03 mL, 0.3 mmol) in MeOH (10 mL) was added a catalyst (30 mg). The reaction mixture was stirred for 12 h at rt. The catalyst was removed by filtration. After evaporation of the solvent, the residue was analyzed by ^1H NMR spectroscopy.

RESULTS AND DISCUSSION**Synthesis and Characterization**

The ADA was synthesized from an ethynyl-functionalized adamantane derivative and 2,5-dibromoterephthalic acid through Sonogashira–Hagihara cross-coupling. A slight excess amount of the ethynyl-functionalized adamantane monomer with respect to 2,5-dibromoterephthalic acid was used because of side reactions such as homocoupling between ethynyl groups.¹⁰ ADA had two carboxyl groups which could be utilized for Yb(III) coordination. Under basic conditions, the carboxyl group was deprotonated and the resulting carboxylate was reacted with Yb(III) chloride hexahydrate to form a Yb(III) complex. A synthetic pathway of ADA and Yb(III)-coordinated ADA (Yb-ADA) is shown in Scheme 1.

The incorporation of Yb(III) ions in ADA was confirmed by XPS measurements. The O 1s and C 1s peaks appeared at



SCHEME 1 Synthesis of ADA and Yb-ADA.

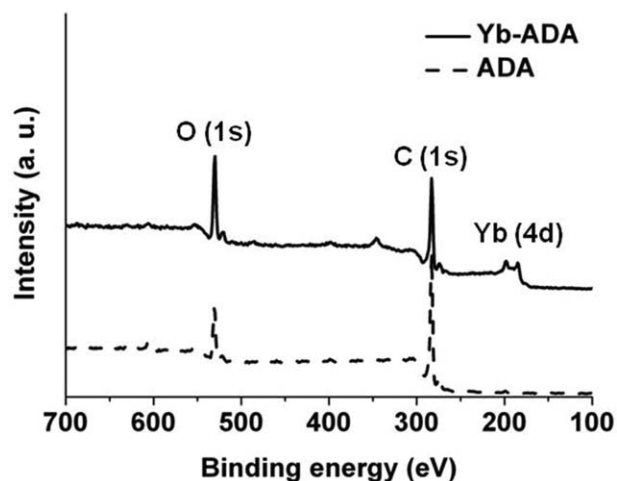


FIGURE 1 XPS spectra of ADA and Yb-ADA.

the binding energy of 530 and 283 eV, respectively in ADA (Fig. 1). After coordination with Yb(III), the polymer (Yb-ADA) emitted Yb 4d photoelectrons with the corresponding binding energy at 185 eV in addition to O 1s and C 1s photoelectrons. The Cl 2p photoelectrons were also detected at 198 eV because an Cl anion could remain as a counter ion for Yb(III). On the assumption that Yb(III) ions were distributed homogeneously in Yb-ADA, we estimated atomic ratios of C, O, and Yb using XPS elemental analysis. The ratio of C:O:Yb was found to be 86.36:13.64:0 in ADA and 69.88:27.79:2.33 in Yb-ADA. The concentration of Yb was smaller than the value calculated from the ideal structure probably because various coordination structures could be formed. The XPS elemental analysis results and theoretical compositions are summarized in Table 1.

Figure 2 shows the ^{13}C NMR spectra of ADA and Yb-ADA. In ADA, the carbon peaks from the carboxyl and ethynyl groups appeared at 165 and 80 ppm, respectively. The peak for aromatic carbons adjacent to the adamantane ring appeared at 149 ppm and the peaks for other aromatic carbons appeared at 130 and 123 ppm. The adamantane carbon peaks were shown at 38 and 44 ppm. All these peaks were also

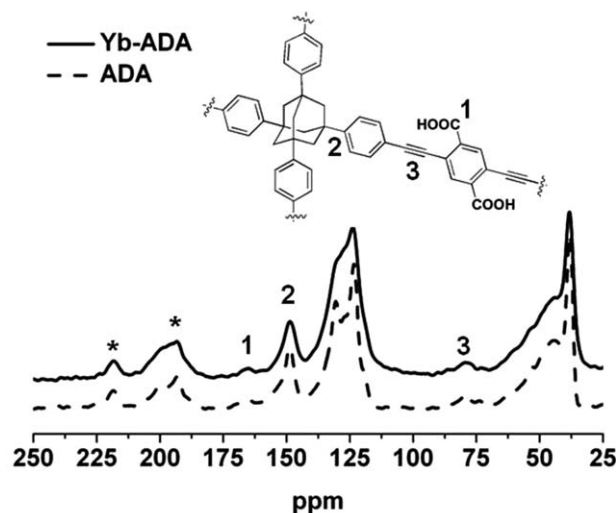


FIGURE 2 Solid-state ^{13}C NMR spectra of ADA and Yb-ADA. The asterisk marks a rotational sideband.

observed in Yb-ADA, indicating that the ADA structure was preserved while coordinated.

Thermal properties of ADA and Yb-ADA were investigated by TGA (Fig. 3). Both ADA and Yb-ADA were thermally stable up to 200 °C and degraded gradually as the temperature increased further. ADA and Yb-ADA had char yields of 65 and 73 wt %, respectively at 800 °C. The higher char yield of Yb-ADA could be caused by the coordinated Yb(III) ions.

Gas Adsorption Properties

The N_2 adsorption/desorption isotherms and pore distributions of ADA and Yb-ADA are shown in Figure 4. The Brunauer-Emmett-Teller (BET) surface area of ADA calculated from the N_2 adsorption isotherm at 77 K was $970 \text{ m}^2 \text{ g}^{-1}$. As the Yb(III) ions were incorporated into ADA, the surface area of the polymer (Yb-ADA) was reduced to $885 \text{ m}^2 \text{ g}^{-1}$. The incorporation of Yb(III) ions into ADA also appeared to change the pore size distribution when calculated by

TABLE 1 Atomic Composition of ADA and Yb-ADA Determined by XPS

Polymer		Atomic Composition (%)		
		C	O	Yb
ADA	Theoretical ^a	88.57	11.43	–
	XPS analysis	86.36	13.64	–
Yb-ADA	Theoretical ^a	68.89	26.67	4.44
	XPS analysis	69.88	27.79	2.33

^a Theoretical values were calculated on the assumption that all ethynyl groups were participated in the coupling reaction and Yb(III) was coordinated with one carboxylate group.

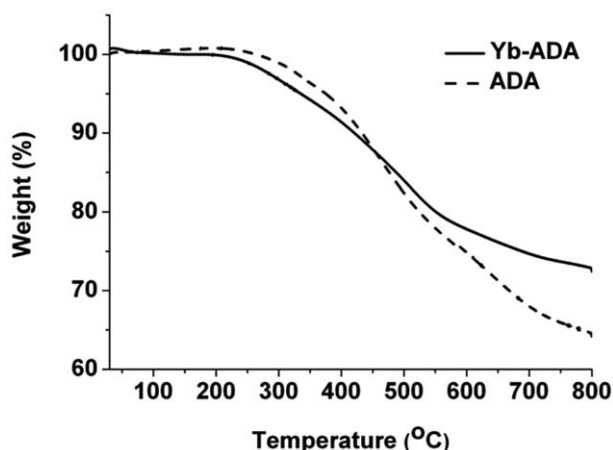


FIGURE 3 TGA thermograms of ADA and Yb-ADA.

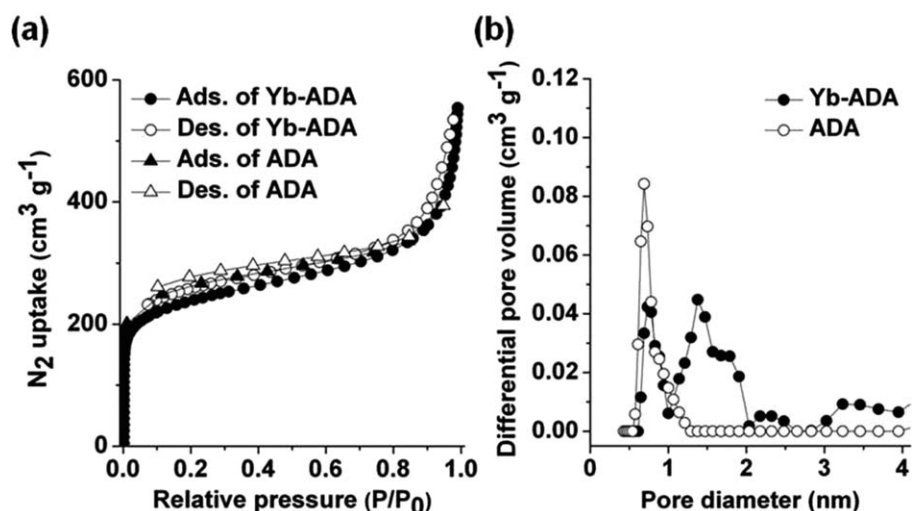


FIGURE 4 N_2 adsorption/desorption isotherms at 77 K for ADA and Yb-ADA (a) and their pore size distributions calculated using NLDFT (b).

nonlocal density function theory (NLDFT) with a cylindrical model. Given the calculation, the proportion of ultrafine micropores (<1 nm) was reduced after coordination and larger micropores were observed more in Yb-ADA. One possible explanation for this result was that the pore structure was changed by coordination and deviated from the cylindrical model. The micropore volume decreased from 0.36 to 0.34 $\text{cm}^3 \text{g}^{-1}$ after coordination, leading to the surface area decrease.

The CO_2 adsorptions were measured up to 1 bar at 273 and 298 K [Fig. 5(a)]. ADA showed the CO_2 adsorption of 2.57 and 1.56 mmol g^{-1} at 273 and 298 K, respectively. Yb-ADA exhibited significantly enhanced CO_2 adsorption capacity of 3.49 and 2.36 mmol g^{-1} at 273 and 298 K, respectively even though it had a smaller surface area compared to ADA. This result was attributable to the fact that the cationic open

metal sites of Yb(III) interacted with CO_2 electrostatically.¹¹ The interaction between Yb(III) and CO_2 was further proved by the heat of adsorption measurement [Fig. 5(b)]. The heat of adsorption was obtained from the CO_2 adsorption isotherms at 273 and 298 K. Yb-ADA showed a larger initial heat of adsorption (31.7 kJ mol^{-1}) than ADA (28.5 kJ mol^{-1}).

The capture of CO_2 from flue gas is of great interest because CO_2 is considered one of the main causes of global warming. Flue gas usually comprises mostly nitrogen and about 15% CO_2 .¹² Accordingly, the high selectivity of CO_2 over N_2 at low pressures is essential for the efficient separation of CO_2 in flue gas. The initial CO_2 and N_2 adsorption isotherms at 298 K are compared in Figure 6. The comparison of initial adsorptions has been reasonably used to investigate the interaction between a gas and a porous polymer while

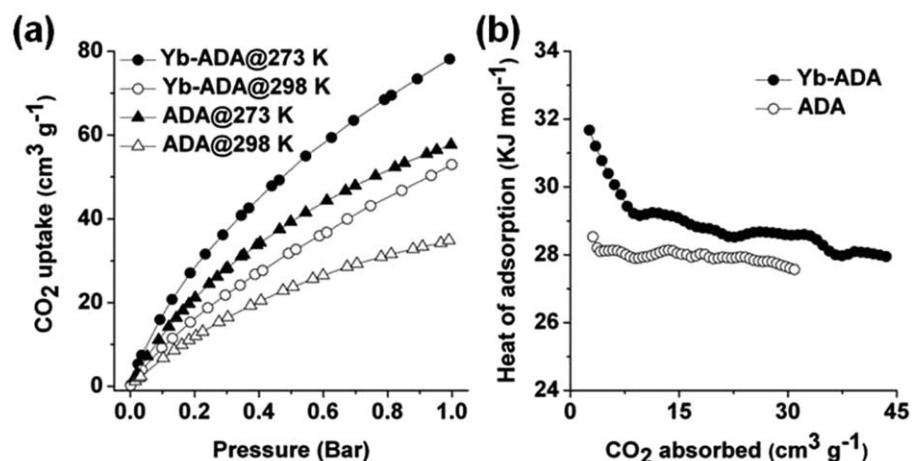


FIGURE 5 CO_2 adsorptions at 273 and 298 K for ADA and Yb-ADA (a) and their isosteric heats of adsorption for CO_2 (b).

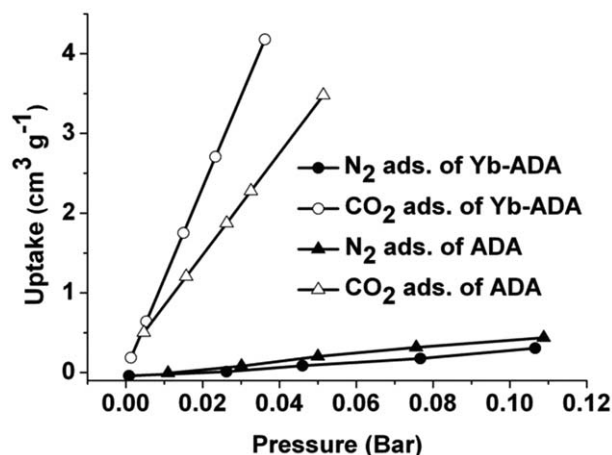


FIGURE 6 CO₂ and N₂ adsorption isotherms of ADA and Yb-ADA at 298 K within the pressure range of 0.0–0.1 bar.

excluding other factors such as gas-gas interactions and pore shapes.¹³ The CO₂ and N₂ adsorption isotherms showed linear slopes within the pressure range of 0.0–0.1 bar. The initial CO₂ adsorption slope of Yb-ADA was steeper than that of ADA, while two polymers showed a similar initial slope in

the N₂ adsorption. The selectivity of CO₂ over N₂ was calculated based on the initial uptake slopes. The CO₂/N₂ selectivity of Yb-ADA was 38, which was 2.7 times higher than that of ADA (14).

Figure 7 shows the H₂ adsorption isotherms at 77 and 87 K. The H₂ uptake of ADA also increased after coordination with Yb(III) from 1.15 to 1.40 wt % at 77 K and from 0.81 to 0.95 wt % at 87 K. The initial heats of adsorption of Yb-ADA and ADA, calculated from adsorption isotherms at 77 and 87 K, were 11.5 and 7.7 kJ mol^{−1}, respectively. The CO₂ and H₂ adsorption properties of the polymers are summarized in Table 2.

Catalytic Activity

The catalytic activity of ADA and Yb-ADA in a condensation reaction was investigated. We used an acetal formation reaction of 4-bromobenzaldehyde and furfural with trimethyl orthoformate as a model reaction. ADA with catalytic carboxyl groups produced acetals in very low yields of 5% and 28 % for 4-bromobenzaldehyde and furfural, respectively. In contrast, in the presence of Yb-ADA, 4-bromobenzaldehyde and furfural were completely converted to the corresponding

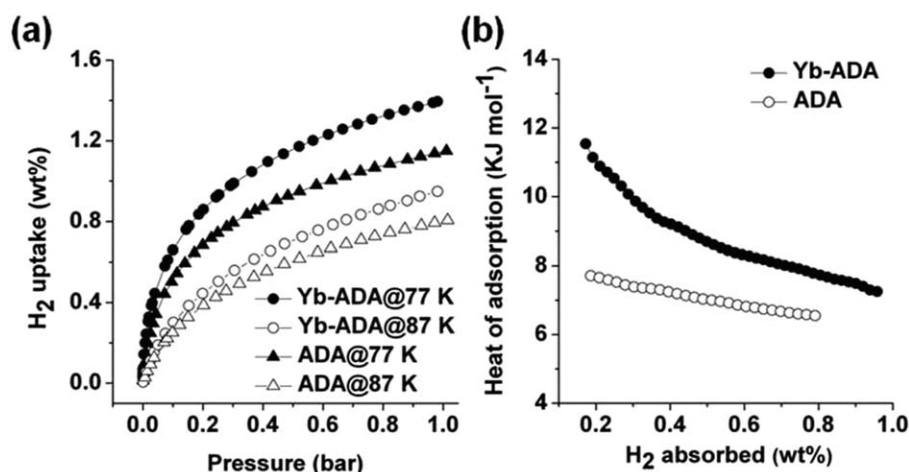


FIGURE 7 H₂ adsorption isotherms at 77 and 87 K for ADA and Yb-ADA (a) and their isosteric heats of adsorption for H₂ (b).

TABLE 2 Surface Areas, Pore Volumes, and CO₂ and H₂ Uptakes of ADA and Yb-ADA

Polymer	S_{BET} (m ² g ^{−1}) ^a	V_{micro} (cm ³ g ^{−1}) ^b	V_{total} (cm ³ g ^{−1}) ^b	$V_{0.1/\text{total}}$	CO ₂ uptake at 1 bar (mmol g ^{−1}) ^c	H ₂ uptake at 1 bar (wt %) ^d
ADA	970	0.36	0.82	0.44	2.57 (1.56)	1.15 (0.81)
Yb-ADA	885	0.34	0.85	0.40	3.49 (2.36)	1.40 (0.95)

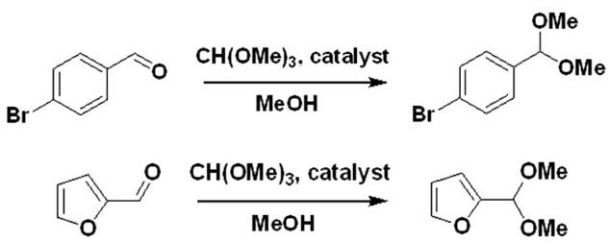
^a Surface areas were calculated by the BET method from N₂ adsorption isotherms at 77 K.

^b Micropore volume and total pore volume were determined at $P/P_0 = 0.1$ and $P/P_0 = 0.995$, respectively.

^c CO₂ uptakes measured at 273 K and at 298 K in parenthesis.

^d H₂ uptakes measured at 77 K and 87 K in parenthesis.

TABLE 3 Conversion Yields in Acetalization of 4-Bromobenzaldehyde and Furfural^a

		
Catalyst	4-Bromobenzaldehyde	Furfural
Without the catalyst	0	0
ADA	5	28
Yb-ADA	100	100

^a The reaction conditions were same except the catalyst.^b Conversion yields were determined by ¹H NMR spectroscopy.

acetals under the same reaction conditions. Without the polymers, the reaction did not occur (Table 3). Yb-ADA was reused five times consecutively in the acetalization of 4-bromobenzaldehyde and furfural. Conversion yields were almost retained, implying that Yb-ADA as a heterogeneous catalyst could be reused after recovery without severe loss of activity (Fig. 8).

CONCLUSIONS

We reported the synthesis of the ADA containing Yb(III) ions by post-coordination. The polymer showed the enhancement of gas adsorption and catalytic activity in acetalization. Following the inclusion of Yb(III) ions, CO₂ uptake of the polymer was enhanced by about 50% at 298 K and H₂ uptake by 21% at 77 K. The Yb(III)-coordinated polymer also func-

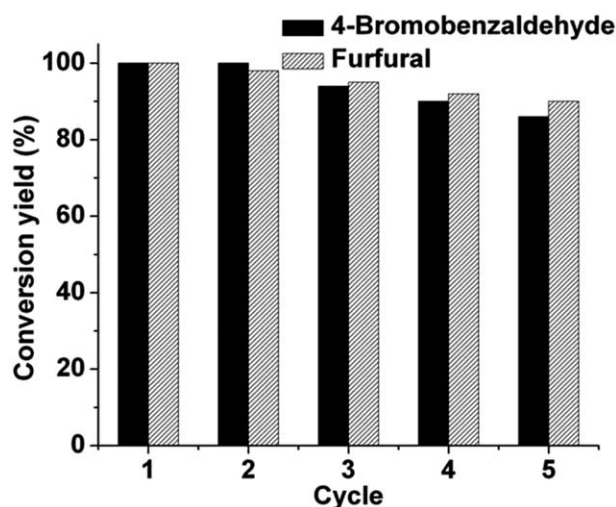
tioned as a heterogeneous catalyst in acetalization. These results suggested that cationic open metal sites of Yb(III) in the polymer strongly interacted with electron rich parts of H₂ and CO₂ for adsorption, and with an unshared electron pair on the oxygen atom for catalysis. This work demonstrates that the introduction of metal ions of interest into MOPs is an efficient way to further optimize their properties.

ACKNOWLEDGMENTS

This research was supported by grants from the Mid-career Researcher Program through NRF grant (No. 2010-0017552) funded by the Ministry of Education, Science, and Technology.

REFERENCES

- (a) N. B. McKeown, P. M. Budd, *Macromolecules* **2010**, *43*, 5163–5176; (b) J. R. Holst, A. I. Cooper, *Adv. Mater.* **2010**, *22*, 5212–5216; (c) R. Dawson, A. I. Cooper, D. J. Adams, *Prog. Polym. Sci.* **2012**, *37*, 530–563; (d) D. Wu, F. Xu, B. Sun, R. Fu, H. He, K. Matyjaszewski, *Chem. Rev.* **2012**, *112*, 3959–4015.
- (a) H. Lim, M. C. Cha, J. Y. Chang, *Polym. Chem.* **2012**, *3*, 868–870; (b) H. Lim, M. C. Cha, J. Y. Chang, *Macromol. Chem. Phys.* **2012**, *213*, 1385–1390; (c) H. Lim, J. Y. Chang, *Macromolecules* **2010**, *43*, 6943–6945; (d) B. Li, R. Gong, W. Wang, X. Huang, W. Zhang, H. Li, C. Hu, B. Tan, *Macromolecules* **2011**, *44*, 2410–2414; (e) Y. Yampolskii, *Macromolecules* **2012**, *45*, 3298–3311; (f) S.-Y. Moon, H.-R. Mo, M.-K. Ahn, J.-S. Bae, E. Jeon, J.-W. Park, *J. Polym. Sci. Part A: Polym. Chem.* **2013**, *51*, 1758–1766; (g) J. Germain, J. M. J. Fréchet, F. Svec, *Small* **2009**, *5*, 1098–1111; (h) R. Dawson, A. I. Cooper, D. J. Adams, *Polym. Int.* **2013**, *62*, 345–352.
- (a) W. Lu, D. Yuan, J. Sculley, D. Zhao, R. Krishna, H.-C. Zhou, *J. Am. Chem. Soc.* **2011**, *133*, 18126–18129; (b) R. Dawson, D. J. Adams, A. I. Cooper, *Chem. Sci.* **2011**, *2*, 1173–1177; (c) S. Ren, R. Dawson, A. Laybourn, J.-X. Jiang, Y. Khimyak, D. J. Adams, A. I. Cooper, *Polym. Chem.* **2012**, *3*, 928–934; (d) R. Dawson, T. Ratvijitvech, M. Corker, A. Laybourn, Y. Z. Khimyak, A. I. Cooper, D. J. Adams, *Polym. Chem.* **2012**, *3*, 2034–2038; (e) N. Shanmugam, K.-T. Lee, W.-Y. Cheng, S.-Y. Lu, *J. Polym. Sci. Part A: Polym. Chem.* **2012**, *50*, 2521–2526; (f) H. Yu, C. Shen, M. Tian, J. Qu, Z. Wang, *Macromolecules* **2012**, *45*, 5140–5150.
- (a) D. Cao, J. Lan, W. Wang, B. Smit, *Angew. Chem. Int. Ed.* **2009**, *48*, 4730–4733; (b) H. Ma, H. Ren, X. Zou, F. Sun, Z. Yan, K. Cai, D. Wang, G. Zhu, *J. Mater. Chem. A* **2013**, *1*, 752–758; (c) A. Li, R.-F. Lu, Y. Wang, X. Wang, K.-L. Han, W.-Q. Deng, *Angew. Chem. Int. Ed.* **2010**, *49*, 3330–3333.
- (a) L. Chen, Y. Yang, D. Jiang, *J. Am. Chem. Soc.* **2010**, *132*, 9138–9143; (b) L. Chen, Y. Yang, Z. Guo, D. Jiang, *Adv. Mater.* **2011**, *23*, 3149–3154; (c) Z. Xie, C. Wang, K. E. deKrafft, W. Lin, *J. Am. Chem. Soc.* **2011**, *133*, 2056–2059; (d) J.-X. Jiang, C. Wang, A. Laybourn, T. Hasell, R. Clowes, Y. Z. Khimyak, J. Xiao, S. J. Higgins, D. J. Adams, A. I. Cooper, *Angew. Chem. Int. Ed.* **2011**, *50*, 1072–1075; (e) K. Thiel, R. Zehbe, J. Roeser, P. Strauch, S. Enthaler, A. Thomas, *Polym. Chem.* **2013**, *4*, 1848–1856; (f) J. Lei, D. Li, H. Wang, Z. Wang, G. Zhou, *J. Polym. Sci. Part A: Polym. Chem.* **2011**, *49*, 1503–1507; (g) Y. Morisaki, M. Gon, Y. Chujo, *J. Polym. Sci. Part A: Polym. Chem.* **2013**, *51*, 2311–2316.
- (a) R. B. Getman, J. H. Miller, K. Wang, R. Q. Snurr, *J. Phys. Chem. C* **2011**, *115*, 2066–2075; (b) B. Mu, P. M. Schoenecker, K. S. Walton, *J. Phys. Chem. C* **2010**, *114*, 6464–6471.

**FIGURE 8** Conversion yields of Yb-ADA in five cycles of acetalization.

- 7** (a) S. Kobayashi, M. Sugiura, H. Kitagawa, W. W.-L. Lam, *Chem. Rev.* **2002**, *102*, 2227–2302; (b) J. Inanaga, H. Furuno, T. Hayano, *Chem. Rev.* **2002**, *102*, 2211–2225; (c) H. C. Aspinall, J. F. Bickley, N. Greeves, R. V. Kelly, P. M. Smith, *Organometallics* **2005**, *24*, 3458–3467.
- 8** (a) L. Yu, D. Chen, J. Li, P. G. Wang, *J. Org. Chem.* **1997**, *62*, 3575–3581; (b) A. Dondoni, A. Massi, *Tetrahedron Lett.* **2001**, *42*, 7975–7978.
- 9** W. Lu, D. Yuan, D. Zhao, C. I. Schilling, O. Plietzsch, T. Muller, S. Bräse, J. Guenther, J. Blümel, R. Krishna, Z. Li, H.-C. Zhou, *Chem. Mater.* **2010**, *22*, 5964–5972.
- 10** (a) A. Elangovan, Y.-H. Wang, T.-I. Ho, *Org. Lett.* **2003**, *5*, 1841–1844; (b) J.-X. Jiang, F. Su, A. Trewin, C. D. Wood, H. Niu, J. T. A. Jones, Y. Z. Khimyak, A. I. Cooper, *J. Am. Chem. Soc.* **2008**, *130*, 7710–7720.
- 11** (a) W. R. Lee, D. W. Ryu, J. W. Lee, J. H. Yoon, E. K. Koh, C. S. Hong, *Inorg. Chem.* **2010**, *49*, 4723–4725; (b) L. Pan, K. M. Adams, H. E. Hernandez, X. Wang, C. Zheng, Y. Hattori, K. Kaneko, *J. Am. Chem. Soc.* **2003**, *125*, 3062–3067; (c) Z. Lin, R. Zou, W. Xia, L. Chen, X. Wang, F. Liao, Y. Wang, J. Lin, A. K. Burrell, *J. Mater. Chem.* **2012**, *22*, 21076–21084.
- 12** (a) D. M. D'Alessandro, B. Smit, J. R. Long, *Angew. Chem. Int. Ed.* **2010**, *49*, 6058–6082; (b) T. C. Drage, C. E. Snape, L. A. Stevens, J. Wood, J. Wang, A. I. Cooper, R. Dawson, X. Guo, C. Satterley, R. Irons, *J. Mater. Chem.* **2012**, *22*, 2815–2823.
- 13** (a) M. G. Rabbani, H. M. El-Kaderi, *Chem. Mater.* **2012**, *24*, 1511–1517; (b) J. An, S. J. Geib, N. L. Rosi, *J. Am. Chem. Soc.* **2010**, *132*, 38–39; (c) R. Banerjee, H. Furukawa, D. Britt, C. Knobler, M. O'Keeffe, O. M. Yaghi, *J. Am. Chem. Soc.* **2009**, *131*, 3875–3877.